CRITICAL HYDRAULIC HEAD LOSS ASSESSMENT FOR A CIRCULAR SHEET PILE WALL UNDER AXISYMMETRIC SEEPAGE CONDITIONS

FARID BOUCHELGHOUM, NAIMA BENMEBAREK

Department of Civil and Hydraulic Engineering, Civil Engineering Laboratory, Biskra University, BP 145 Biskra 07000, Algeria.
E-mail: fbou60@yahoo.fr; benmebarekn@yahoo.fr

Abstract: On excavating soil in areas with a high groundwater level (cofferdam driven in permeable soils in river and maritime sites) seepage of water is a problem. In the design of the cofferdam, various flow conditions should be specified correctly, and the critical hydraulic head difference against seepage failure, H_c, must be estimated exactly. Although several methods have been proposed in the literature, they lead sometimes to great differences in the hydraulic head loss inducing failure. In this paper, the seepage failure problem of homogeneous (isotropic and anisotropic) and problem of multi-layered and isotropic sandy soil under axisymmetric flow conditions are mainly considered and analyzed using an explicit finite difference method implanted in the FLAC2D (Fast Lagrangian Analysis of Continua) Code. Various parameters affecting the stability of the cofferdam were examined. It was found that the effect of *excavation shapes*; *soil anisotropy* and *non-homogeneity* is significant for the reduction of the critical hydraulic head loss H/f corresponding to the zero effective passive earth pressure.

NOMENCLATURE

φ	– angle of internal friction of the soil
ψ	– dilation angle of the soil
γ'	– submerged unit weight of the soil
δ	– angle of friction at the soil/wall interface
γ_w	– unit weight of water
c	– soil cohesion
f	– penetration depth of the sheet pile
H	– total hydraulic head loss
D	– layer depth
B	– diameter of cylindrical cofferdam
n	– porosity
i_c	– critical hydraulic gradient
i_e	– exit gradient
i_m	– average hydraulic gradient along the prism
K	– bulk modulus of the soil
G	– shear modulus of the soil
K_n	– interface normal stiffness
K_s	– interface shear stiffness
K_1, K_2	– isotropic permeability coefficients of layers 1 and 2
K_h, K_v	– horizontal and vertical permeability coefficients

1. INTRODUCTION

In the practice of geotechnical engineering, the seepage of water through the retained soil mass is one of the major factors which influence the design of the retaining structures. The water seepage may change the value and distribution of the passive earth pressure, such that it also influences the stability of such structures. The design of deep excavations is often dominated by the water flow around sheet piles or propped walls. When the hydraulic head difference between the up- and downstream sides, H, is too large, seepage failure occurs at the base of the excavation. The seepage flow influences the stability of the walls where bulk heave, piping or failure by reduction of the earth pressure may occur. In practice, we encounter various types of excavation using single or double sheet pile walls, and various shapes of excavation, e.g., long and narrow, rectangular, square, or circular shapes in a plan view. In recent years, large scale or deep excavation is also encountered.

On excavating a large area, the seepage failure of soil in front of a sheet pile wall is a problem in two dimensions. The influence of seepage flow on the stability of retaining excavations was first addressed by TERZAGHI (1943) [1]. Several methods and model tests have been proposed for assessing the risk of failure due to seepage forces (TERZAGHI 1943 [1]; TERZAGHI and PECK 1948 [2]; McNAMEE 1949 [3]; MARSLAND 1953 [4]; DAVIDENKOFF 1954 [5]; BAZANT 1963 [6]; DAVIDENKOFF and FRANKE 1965 [7]; KASTNER 1982 [8]; KHAN et al. 2001 [9]; BENMEBAREK et al. 2005a [10], 2005b [11]; WUDTKE 2008 [12]). The computation of 2D earth pressures, including active and passive, for retaining wall attracted special attention from TERZAGHI (1943) [1]; HOULSBY (1975) [13]; SOUBRA et al. (1992) [14], (1999) [15]; BENMEBAREK et al. (2006) [16]; WANG et al. (2008) [17].

In the excavation of soil between double sheet pile walls, seepage water concentrates into the soil two-dimensionally from the outside. The two-dimensional concentrated flow of water lowers the safety factor regarding the seepage failure of soil (BAUER 1984 [18]; TANAKA et al. 2002 [19], 2006 [20], 2009 [21]).

When the longitudinal length of the double sheet pile walls is small, seepage flow concentrates three-dimensionally into soil surrounded by a rectangular wall. An axisymmetric seepage flow through soil within a cylindrical wall is often used to model such a three-dimensional flow. The cylindrical wall condition brings about axisymmetrically concentrated flow. The axisymmetrically concentrated flow condition further lowers the safety factor for seepage failure (MIURA 2000 [22]; TANAKA et al. 2002 [19], 2006 [20], 2009 [21]; BOUCHELGHOUM et al. 2007 [23], 2008a [24]). In recent research, LIU et al. (2008) [25] investigated the axisymmetric active earth pressure for layered backfills using the slip line method. Their results indicate that the major principal direction, as well as the earth pressure, has a finite jump on passing the soil interfaces.

The three-dimensional effect of water flow around excavations increases the water pressure to make failure occur easily. Thus the water pressure of three-di-

mensional analysis of water flow around excavations should be used to predict piping or heaving in design if the excavation length is not large enough to consider the excavation as a two-dimensional case (TANAKA et al. 2002 [19], 2009 [21]; BOUCHELGHOUM et al. 2006 [26], 2008b [27]). While the boiling takes place at the excavation level, the heaving is more spectacular and catastrophic. A 3D passive earth pressure study was proposed by SOUBRA (2000) [28]; BENMEBAREK et al. (2008) [29]. Some case histories have indicated that piping occurred though it was considered to be safe based on the two-dimensional methods (CAI et al. 2003 [30], 2004 [31]; KIM, 2005 [32]; TANAKA et al. 2003 [33], 2006 [20]). There are many published methods for the assessment of bottom stability against seepage failure of soil, but failure sometimes occurs even in deep excavation designed by these methods (TANAKA, 2002 [19]). Generally, these methods did not consider the influence of the excavation shape on the critical hydraulic head loss causing failure. Therefore more precise analysis is required to clarify the failure mechanisms.

In this context, to investigate the influence of seepage flow on stability of the axisymmetric excavation bottom, axisymmetric numerical analysis has been carried out using the code FLAC2D [34] (Fast Lagrangian Analyses of Continua in two-Dimensions) for better understanding the seepage failure phenomena. From a series of numerical experiments, it is found that the failure mechanism shapes and the hydraulic head loss at failure are significantly influenced by: soil and interface characteristics; anisotropy of the permeability coefficient; and are very sensitive to the layered permeability ratio. The axisymmetric effect makes the critical hydraulic head loss causing failure lower than that of two-dimensional methods. This is just the reason why failure took place in the excavations that were considered to be safe based on two-dimensional methods.

2. TERZAGHI'S WORK

The influence of seepage flow on the stability of retaining excavations was first addressed by TERZAGHI (1943) [1]. From model tests, he found that within an excavation, the zone of danger of bottom heave is confined to a soil prism adjacent to the wall. He assumed, from experimental evidence, that the body of sand, which is lifted by water, has the shape of a rectangular prism (Fig. 1) with a width equal to half the wall penetration $D/2$ and the horizontal base at some depth D_0 below the surface ($0 \leq D_0 \leq D$). It is assumed that at the instant of failure, the effective horizontal stresses on the prism vertical sides and the corresponding frictional resistance are zero. Therefore, the prism rises up and collapses as soon as the total excess water pressure U_e on the bottom of the prism OA becomes equal to the submerged weight of the prism W'.

The safety factor against bulk heave is determined by the ratio of the submerged weight of the prism to the excess water force on the prism base:

$$F_s = W'/U_e = i_c/i_m \qquad\qquad (1)$$

where i_m is the average hydraulic gradient between *IJ* and *EF*.
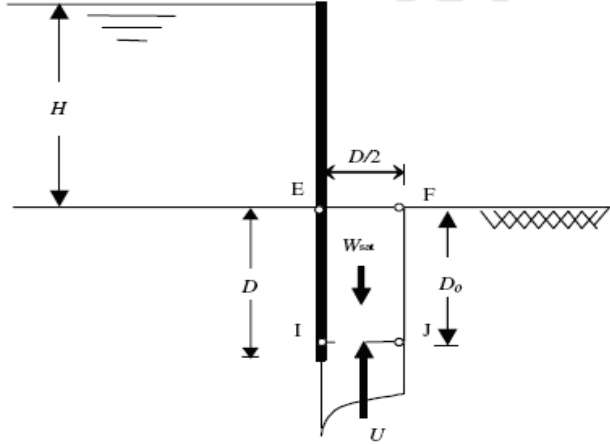

Fig. 1. Failure by heaving (after TERZAGHI 1943 [1])

3. NUMERICAL MODELLING PROCEDURE

3.1. CASES STUDY

This paper deals with the numerical study of bottom stability against seepage failure of sand within cylindrical cofferdam. First, we consider a sheet pile with penetration depth equal to f in homogeneous (isotropic and anisotropic) semi-infinite and finite soil ($D/f = 2$), with D layer depth, $B/2$ radius of the cylindrical cofferdam, which is subjected to hydraulic head H, as shown in Fig. 2. Due to the axisymmetry, only one half of the model is analyzed. This problem has many parameters: excavation or cofferdam width (diameter), penetration of retaining wall in the soil, thickness of permeable soil, wall flexibility, strut rigidity, wall translation and rotation, etc.

The objective of this work is not to consider the influence of all these parameters but to check if a numerical analysis using the finite difference or the finite element approach can describe correctly the various failure mechanisms observed due to upward seepage flow into a cylindrical cofferdam. Therefore, the problem has been simplified by referring to some model test observations of failures and to the classical approaches where the action of the wall on the soil is not directly considered, but the wall is being considered as fixed.

An infinite rigid wall is considered in this study. This is a simplification of the real problem where the wall flexibility leads to a limited partial support of the soil on the

wall embedment. This allows us to show the presence of the supposed fixed wall ef-
fect on the failure mechanisms as well as the comparison of the results with the classi-
cal approaches where the wall is taken into account from the hydraulic point of view
only. The analysis is carried out using the computer code FLAC2D which is a com-
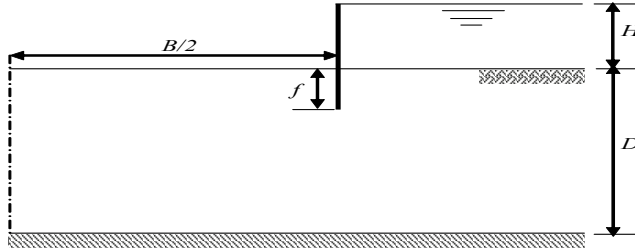mercially available finite difference explicit program.

Fig. 2. Case of homogeneous medium

The soil behaviour is modelled by the elastic-perfectly plastic nonassociative
Mohr–Coulomb model encoded in Flac2D code. All subsequent results are given for
saturated weight of soil γ_{sat} and unit weight of water γ_w as: $\gamma_{sat}/\gamma_w = 2$, elastic bulk
modulus $K = 30$ MPa and shear modulus $G = 11.25$ MPa. Four values of the angle of
internal friction $\varphi = 20°, 30°, 35°, 40°$, four values of the friction angle at the soil/wall
interface $\delta/\varphi = 0, 1/3, 2/3, 1$, and three values of the dilation angle $\psi/\varphi = 0, 1/2, 1$ are
considered in the analysis.

3.2. MODELLING PROCEDURE

In the case of a rough wall, modelling the interface between the soil and the wall is
invariably an integral part of the analysis. The material properties, particularly stiff-
ness assigned to an interface, depend on the way in which the interface is used. In the
case of soil–structure interaction, the interface is considered stiff compared to the sur-
rounding soil, but it can slip and may be open in response to the loading. Joints with
zero thickness are more suitable for simulating the frictional behaviour at the interface
between the wall and the soil. The interface model shown in Fig. 3 has been used to
simulate the soil/wall contact described by Coulomb law. The logic contact for either
side of the interface is similar in nature to the interface used in the distinct element
method (CUNDALL and HART 1992 [35]). The spring in the tangential direction and
the slider (Fig. 3) represent the Coulomb shear-strength criterion. The spring in the
normal direction and the limit strength represent the normal contact.

The interface has a friction angle δ, a cohesion $c = 0$ kPa, a normal stiffness $K_n =$
10^9 Pa/m, and a shear stiffness $K_s = 10^9$ Pa/m. These values of K_n and K_s are selected
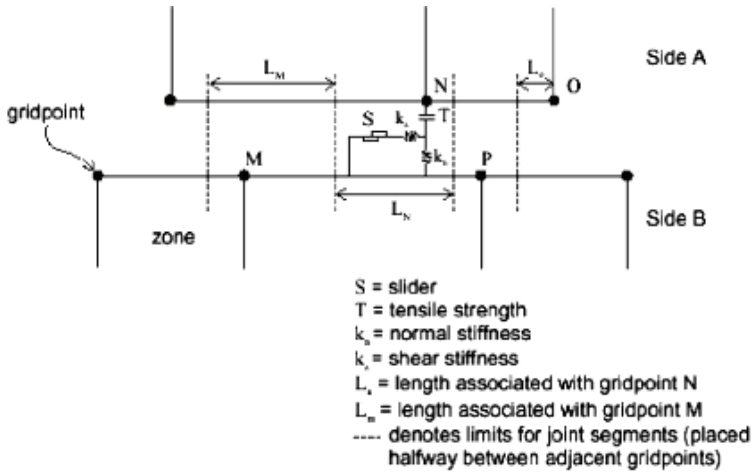to approximate the results for the case where the wall is rigidly attached to the grid.

Fig. 3. Interface element used (Manuel Flac2D)

The prediction of collapse conditions under steady plastic flow conditions is one that can be difficult for a numerical model to simulate accurately (SLOAN and RANDOLPH 1982 [36]). FRYDMAN and BURD (1997) [37], and ERICKSON and DRESHER (2002) [38] operating with viscoplastic or elastoplastic algorithms, have shown clearly the dependence of the plane strain bearing capacity factor N_γ on the geometry of the mesh and indicated the reduction of this factor with decreasing value of soil dilation angle.

Accordingly, in order to develop an acceptable analysis scheme for later computations for the axisymmetric case, preliminary simulations have been carried out by testing the influence of the mesh dimensions, the element size, the boundary conditions and the earth pressure coefficient at rest K_0 as well. The results show the difficulty in the capturing of the failure mechanisms for coarse meshes and prove the requirement of refined mesh to capture it clearly. Also, the results confirm that variation in practical range of the elastic soil parameters and earth pressure coefficient at rest K_0 do not have any significant influence on the critical hydraulic pressure loss, as the numerical estimation of the bearing foundation capacity factor N_γ.

Figure 4 shows the mesh and boundary conditions retained for this analysis. The mesh size is fine near the wall where deformations and flow gradients are concentrated. In order to minimize boundary effects, the length from the wall and the depth of the mesh are respectively located at six times the wall penetration in the case of the semi-infinite medium (the diameter B (Fig. 4) is large enough so that there is no interaction of the two failure mechanisms which develop in front of the two walls of the cofferdam).

As a general rule for the boundary conditions, the bottom boundary is assumed to be fixed; the right and left lateral boundaries are fixed in the horizontal directions.

The sheet piles wall is modelled by quadrilateral massif elements connected to the soil grid via interface elements attached on both sides of the massif elements. The wall thus acts as an impermeable member.
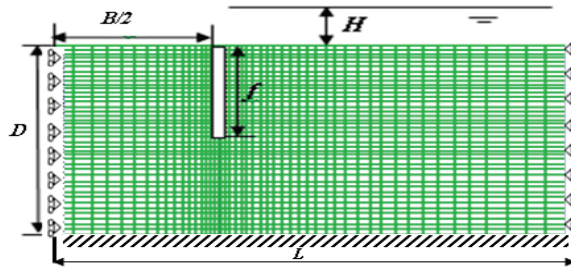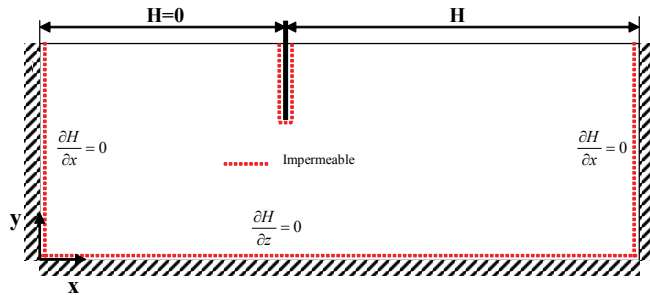

Fig. 4. Mesh used and boundary conditions

Fig. 5. Hydraulic boundary conditions

To identify the limiting cases corresponding to zero passive earth pressures and seepage failure by heaving or boiling, the following three simulation procedure steps are adopted:

1. The geostatic stresses are computed assuming the material to be elastic. The initial pore pressure and effective stresses are established using the Fish library function assuming that the ratio of effective horizontal stress to effective vertical stress at rest is taken $K_0 = 0.5$. The groundwater level is assumed to be located at the ground surface. This analysis is performed within the groundwater configuration as uncoupled groundwater flow and mechanical calculation.

2. The field describing the distribution of the pore water pressure due to a hydraulic head loss H is calculated under hydraulic limit conditions shown in Fig. 5.

3. The mechanical response is investigated for the pore pressure distribution established in the previous step.

Steps 2 and 3 are repeated with the progressive increase of the hydraulic head loss until failure. It is noted that the simulation procedure does not impose a horizontal displacement of the wall as for the computation of the passive earth pressures. It

should be mentioned that the evaluation of the precise value of *H/f* for which the passive pressures vanish is not easy to obtain. Therefore, only the bottom stability against soil seepage failure is investigated for different ranges of the hydraulic head loss *H/f*, various governing parameters soil friction, soil dilation and interface friction.

4. NUMERICAL RESULTS AND DISCUSSION

Notice that the time of calculation of semi-infinite case is longer than for the finite medium, and the calculations taking account of the anisotropy effect increase the time of calculation.

4.1. CASE OF HOMOGENEOUS AND ISOTROPIC SOIL MEDIUM

Results for failure by heaving are presented by one asterisk or two and failure by boiling by three.

Numerical studies are performed for different soil friction angles and the results are presented in Table 1 and Table 2 for $\varphi = 20°, 25°, 30°, 35°$ and $40°$.

Table 1

Critical hydraulic head loss *H/f* for various governing parameters φ, ψ/φ and δ/φ.
Case of semi-infinite medium

φ: degrees	ψ/φ	H/f limit							
		δ/φ							
		0		1/3		2/3		1	
		Flac2D	B	Flac2D	B	Flac2D	B	Flac2D	B
20	0	2.10*	2.63*	2.13*	2.67*	2.17*	2.72*	2.17*	2.73*
	1/2	2.11**	2.64**	2.13**	2.68**	2.17**	2.73**	2.17**	2.73**
	1	2.11**	2.64**	2.13**	2.68**	2.17**	2.73**	2.17**	2.73**
25	0	2.15*	2.68*	2.19*	2.78*	2.19*	2.81*	2.23*	2.84*
	1/2	2.16**	2.70**	2.19**	2.82**	2.21**	2.83**	2.24**	2.87**
	1	2.18**	2.71**	2.20**	2.84**	2.23**	2.84**	2.25**	2.90**
30	0	2.19*	2.74*	2.28*	2.84*	2.28*	2.90*	2.28*	2.90*
	1/2	2.26**	2.79**	2.29**	2.88**	2.30**	2.92**	2.30**	2.94**
	1	2.27**	2.82**	2.30**	2.91**	2.31**	2.93**	2.31**	2.98**
35	0	2.23*	2.77*	2.30*	2.90*	2.30*	2.92*	2.31*	2.93*
	1/2	2.26**	2.82**	2.31**	2.94**	2.33**	2.97**	2.34**	3.03**
	1	2.28***	2.84**	2.32***	2.97**	2.36***	3.04***	2.37***	3.05***
40	0	2.25*	2.80*	2.30*	2.93*	2.32*	2.97*	2.32*	2.99*
	1/2	2.28**	2.90**	2.33**	2.98**	2.35**	3.12**	2.38**	3.13**
	1	2.30***	2.93**	2.35***	3.03**	2.37***	3.16***	2.40***	3.16***

B: after BENMEBAREK et al. (2005a) [10]

Critical hydraulic head loss *H/f* for various governing parameters
φ, ψ/φ and δ/φ. Case of finite medium

δ/φ	ψ/φ	*H/f* limit				
		$\Phi = 20°$	$\Phi = 25°$	$\Phi = 30°$	$\Phi = 35°$	$\Phi = 40°$
0	0	2.45*	2.70*	2.75*	2.80*	2.81*
	1/2	2.50**	2.71**	2.80**	2.85**	2.88**
	1	2.55**	2.72**	2.90**	2.92***	2.94***
1/3	0	2.56*	2.73*	2.78*	2.82*	2.83*
	1/2	2.57**	2.74**	2.92**	2.93**	2.94**
	1	2.57**	2.74**	2.93**	2.94***	2.96***
2/3	0	2.56*	2.73*	2.79*	2.83*	2.84*
	1/2	2.57**	2.74**	2.93**	2.94**	2.96**
	1	2.57**	2.75**	2.94**	2.96***	2.98***
1	0	2.57*	2.74*	2.80*	2.84*	2.86*
	1/2	2.57**	2.75**	2.94**	2.95**	2.97**
	1	2.57**	2.76**	2.95**	2.97***	2.99***

Failure by bulk heave of rectangular (*) or triangular (**) soil prisms, or by boiling (***)

These results indicate clearly that the axisymmetric bottom stability against seepage failure always corresponds to a bulk heave except in the case of a dense sand $\varphi \geq 35°$, a dilating material $\psi/\varphi > 1/2$ and a rough wall $\delta/\varphi \geq 0$ where boiling would occur.

For the case of *semi-infinite* medium, it can be seen that boiling starts from a hydraulic pressure loss of *H/f* = 2.28. This value is small compared to the theoretical critical head loss value *H/f* = 3.14 (for the case of single sheet pile wall driven into homogenous and isotropic semi-infinite soil medium). In this case, the exit hydraulic gradient attains the critical hydraulic gradient value. Figure 6 shows the failure mechanism indicated by the displacement field and the corresponding distribution of maximum shear strain rates obtained in the case of $\varphi = 40°$, $\psi/\varphi = 1$ and $\delta/\varphi = 1$, *H/f* = 2.40 where boiling phenomenon is indicated.

For the case of *finite* medium (Table 2), the boiling starts from a hydraulic pressure loss of *H/f* = 2.92. This value is larger than that of the axisymmetric semi-infinite case. The numerical results obtained from the present simulation have shown that the critical hydraulic pressure loss *H/f* increases with the *D/f* decrease. We considered for the case of finite medium the value of *D/f* = 2.

For $\psi/\varphi = 0$, a rectangular soil prism similar to that obtained by BENMEBAREK et al. (2005a) [10] and that proposed by TERZAGHI (1943) [1] (in the case of single sheet pile) is observed. Figure 7 shows the failure mechanism in the case of $\varphi = 20°$, $\psi/\varphi = 0$ and $\delta/\varphi = 2/3$ and *H/f* = 2.17 where bulk heave of a rectangular soil prism with a width smaller than that of Terzaghi's method (*f*/2) (in the case of single sheet pile) is

observed. However, for dilating material $\psi/\varphi \geq 1/2$, a triangular soil prism is obtained and is similar to that proposed by Rankine & Kastner and that obtained by BENMEBAREK et al. (2005a) [10] (in the case of single sheet pile). As an example, Fig. 8 shows the case of $\varphi = 20°$, $\psi/\varphi = 1$ and $\delta/\varphi = 2/3$, $H/f = 2.17$ where bulk heave of a triangle soil prism is observed.
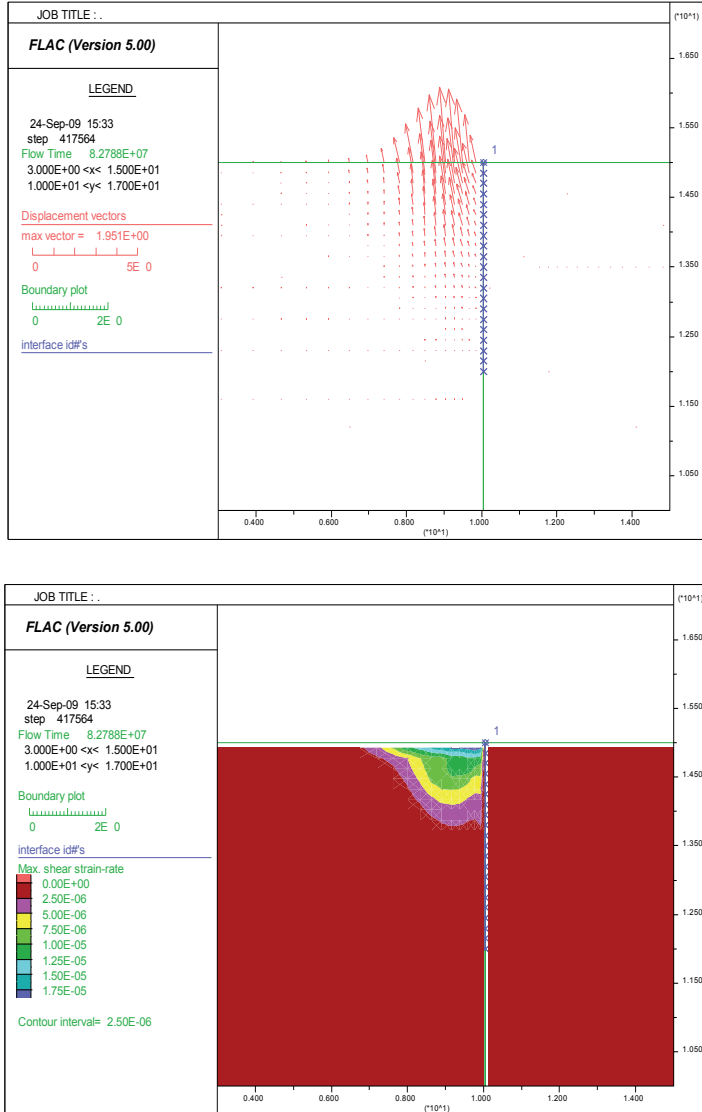

Fig. 6. Displacement field and the corresponding distribution of maximum shear strain rates when $\varphi = 40°$, $\psi/\varphi = 1$, $\delta/\varphi = 1$, $H/f = 2.40$. Semi-infinite medium
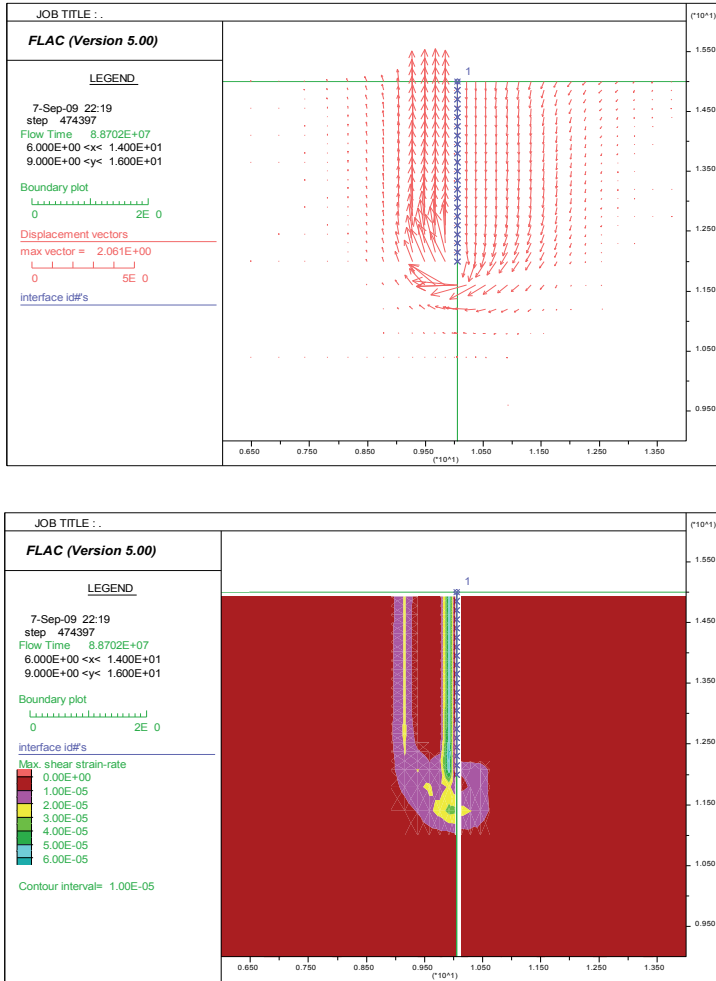
Fig. 7. Displacement field and the corresponding distribution of
maximum shear strain rates when $\varphi = 20°$, $\psi/\varphi = 0$, $\delta/\varphi = 2/3$, $H/f = 2.17$.
Semi-infinite medium

From Table 1, for $\delta/\varphi = 0$, $\psi/\varphi = 1$ and φ varies from 20° to 40°, the critical value of H/f lies in the range of 2.11–2.30. It is noted that for various values of φ in the case of single sheet pile wall driven into homogenous and isotropic semi-infinite medium, BENMEBAREK et al. (2005a) [10] have obtained a value of H/f that lies in the range of 2.64–2.93, Terzaghi's solution is $H/f = 2.82$ whereas that of SOUBRA et al. (1999) [15] solution is $H/f = 2.78$. Therefore, these values of critical hydraulic head loss proposed by these authors are overestimated, and thus the values of the safety factor are overestimated compared to the present axisymmetric case.
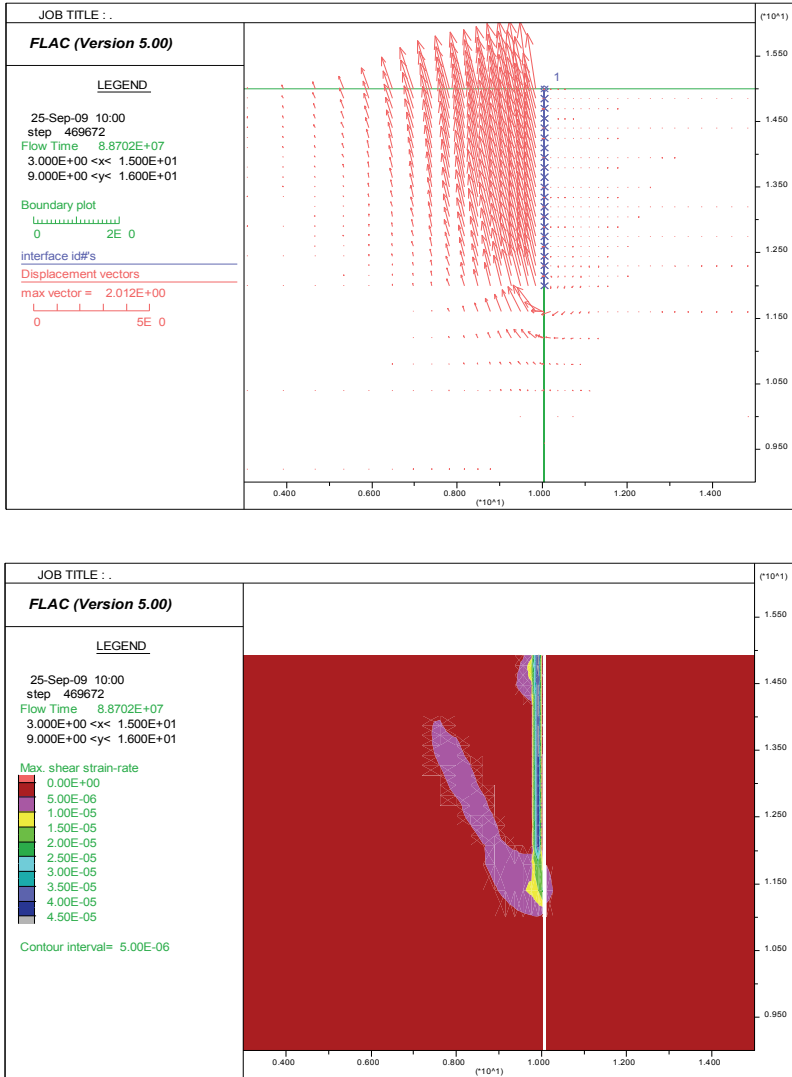
Fig. 8. Displacement field and the corresponding distribution
of maximum shear strain rates when $\varphi = 20°$, $\psi/\varphi = 1$, $\delta/\varphi = 2/3$, $H/f = 2.17$.
Semi-infinite medium

Also, for $\varphi = 40°$, $\psi/\varphi = 1$ and δ/φ varies from 0 to 1, the critical value of H/f lies in the range of 2.30–2.40 whereas that of BENMEBAREK et al. (2005a) [10] 2.93–3.16 (in the case of single sheet pile wall).

The present simulation procedure shows that soil dilation angle has a significant influence on the failure mechanism shape, and contrary to observations noted by

SOUBRA (1992) [14], (1999) [15], this present simulation shows that the angle of friction at the soil/wall interface has a significant influence on the critical hydraulic head loss *H/f* value causing failure by heaving. The present results confirm those obtained by TANAKA (2002) [19]; KHAN et al. (2001) [9].

This behaviour can be explained as follows: when the soil adjacent to the wall expands by dilation at failure, the shear forces induced on the vertical faces of the prism block the rising of the rectangular prism. Therefore, a triangular failure prism appears instead. This corresponds to a kinematically admissible mechanism within the frame of limit analysis theory. This phenomenon has been experimentally observed by KASTNER (1982) [8].

For high values of φ and ψ, shear forces on the wall embedment and horizontal soil expansion by dilation delay the triangular prism failure. Therefore, the surface exit gradient becomes critical before the bulk heave of the triangular prism and initiates the boiling. This case may also occur for a flexible wall supported partially by the soil.

4.2. CASE OF HOMOGENEOUS AND NON-ISOTROPIC SOIL MEDIUM

In reality, permeability is a tensor quantity, with two principal values and two principal directions, in 2D.

Table 3

Critical hydraulic head loss H/f for various governing parameters
φ, ψ/φ and δ/φ in the case of a homogeneous anisotropic semi-infinite medium,
$K_h/K_v = 50$

δ/φ	ψ/φ	H/f limit				
		$\Phi = 20°$	$\Phi = 25°$	$\Phi = 30°$	$\Phi = 35°$	$\Phi = 40°$
0	0	1.67*	1.68*	1.68*	1.69*	1.70*
	1/2	1.68**	1.68**	1.69**	1.70**	1.71**
	1	1.68**	1.68**	1.69**	1.70**	1.71**
1/3	0	1.68*	1.69*	1.70*	1.71*	1.71*
	1/2	1.69**	1.70**	1.71**	1.72**	1.72**
	1	1.69**	1.70**	1.71**	1.72**	1.72**
2/3	0	1.69*	1.70*	1.71*	1.72*	1.72*
	1/2	1.70**	1.71**	1.72**	1.73**	1.73**
	1	1.70**	1.71**	1.72**	1.73**	1.73**
1	0	1.70*	1.70*	1.71*	1.72*	1.73**
	1/2	1.70**	1.71**	1.72**	1.73**	1.74**
	1	1.70**	1.71**	1.72**	1.73**	1.74**

Critical hydraulic head loss H/f for various governing parameters φ, ψ/φ and
δ/φ in the case of a homogeneous anisotropic finite medium ($D/f = 2$), $K_h/K_v = 50$

δ/φ	ψ/φ	H/f limit				
		$\Phi = 20°$	$\Phi = 25°$	$\Phi = 30°$	$\Phi = 35°$	$\Phi = 40°$
0	0	1.42*	1.43*	1.43*	1.44*	1.45*
	1/2	1.43**	1.43**	1.44**	1.45**	1.46**
	1	1.43**	1.43**	1.44**	1.45**	1.46**
1/3	0	1.43*	1.44*	1.45*	1.46*	1.46*
	1/2	1.43**	1.45**	1.46**	1.47**	1.47**
	1	1.44**	1.45**	1.46**	1.47**	1.47**
2/3	0	1.44*	1.45*	1.46*	1.47*	1.47*
	1/2	1.45**	1.46**	1.47**	1.48**	1.48**
	1	1.45**	1.46**	1.47**	1.48**	1.48**
1	0	1.45*	1.45*	1.46*	1.47*	1.48*
	1/2	1.45**	1.46**	1.47**	1.48**	1.49**
	1	1.45**	1.46**	1.47**	1.48**	1.49**

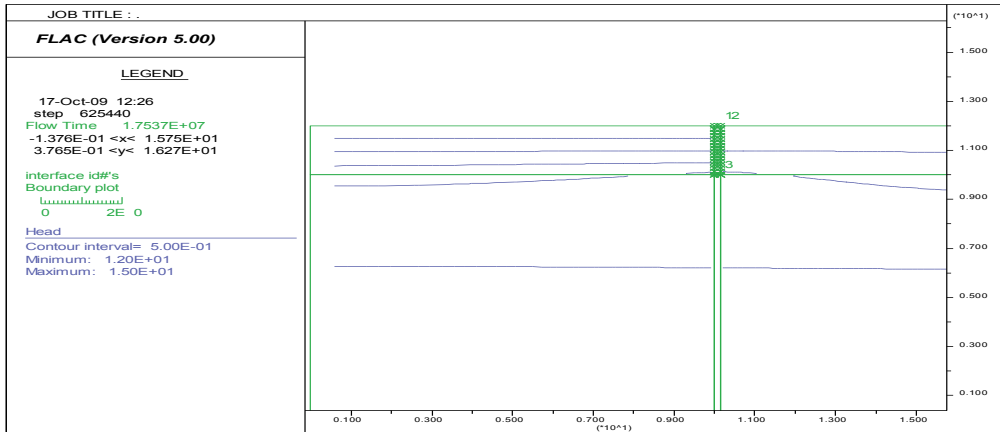Failure by bulk heave of rectangular (*) or triangular (**) soil prisms

Fig. 9. Quasi-horizontal equipotential lines in front of the sheet pile for $H/f = 1.70$.
$\varphi = 40°$, $\psi/\varphi = 0$ and $\delta/\varphi = 0$

These results indicate that the critical hydraulic head loss causing failure H/f is clearly lower than that of isotropic case. Therefore H/f decreases with the increase of the K_h/K_v permeability ratio, since in this case there is a large decrease of the passive earth pressure coefficient and the failure of the adjacent soil of the sheet pile appears for a small hydraulic head loss compared to the isotropic case. This can be explained by the fact that the equipotential lines in front of the sheet pile become quasi-

horizontal beyond a certain value of K_h/K_v and, thus, the potential field does not change any more in the zone concerned with the failure mechanism (Fig. 9).

Otherwise, H/f for the semi-infinite anisotropic medium is larger than that of the finite anisotropic medium. Therefore for anisotropic case, H/f increases with the increase of the relative depth D/f.

These results indicate that contrary to the isotropic case, boiling has not occurred. Hence, the failure mechanism of this anisotropic case defers of the isotropic case. Besides, in anisotropic medium, for high values of φ and ψ, shear forces on the wall embedment and horizontal soil expansion by dilation do not delay the triangular prism failure. Therefore, the surface exit gradient becomes not critical before the bulk heave of the triangular prism and does not initiate the boiling. For $\psi/\varphi = 0$, a rectangular soil prism similar to the axisymmetric isotropic case but with width $>f/2$ is observed. However, for dilating material $\psi/\varphi \geq 1/2$, a triangular soil prism is obtained and is similar to the isotropic case. From Table 3, the critical values of H/f are lower than that of *isotropic* semi-infinite medium case, and larger than that of anisotropic finite medium. The boiling has not occurred. From Table 4, the critical values of H/f are lower than that of isotropic finite medium case.

4.3. CASE OF AN ISOTROPIC TWO-LAYERED SOIL MEDIUM

In this section, we consider the frequent case of cylindrical cofferdam driven into a two-layered soil medium. A sheet pile with penetration depth equal to f in heterogeneous isotropic semi-infinite and finite soil, with D_1 and D_2 thickness of upper and lower layer respectively, B diameter of the cylindrical cofferdam, where the permeability coefficients of the upper and lower layers are respectively K_1 and K_2 which is subjected to hydraulic head H, is considered as shown in Fig. 10 and Fig. 11. Due to the axisymmetry, only one half of the model is analysed.
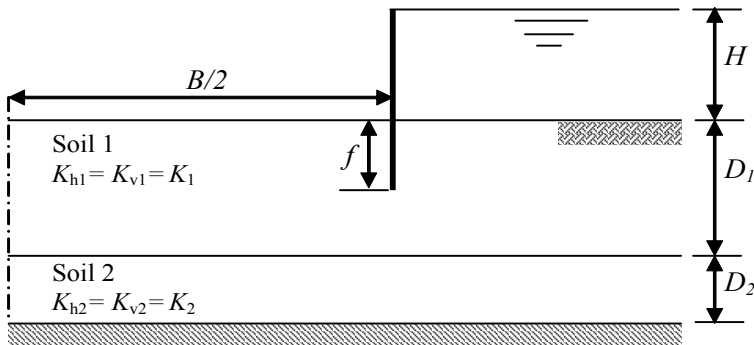

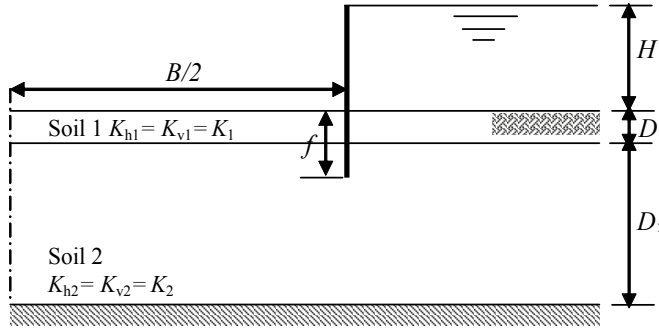Fig. 10. Case of an isotropic two-layered soil medium case A

Fig. 11. Case of an isotropic two-layered soil medium case B

For the case of a single layer ($K_1/K_2 = 1$), the hydraulic head loss H/f is equal to 2.57 for both case A and B in finite medium, and 2.40 for semi-infinite medium. When $K_1/K_2 > 10$ (Fig. 12), or $K_1/K_2 \geq 1$ and $D_1/f \geq 2$ (Fig. 14), one can obtain the hydraulic head loss corresponding to the case of a single layer of limited depth ($\varphi = 35°$, $\delta/\varphi = 2/3$, $H/f = 2.77$, and $D_1/f = 2$), since the lower layer can be considered as an impermeable substratum. Otherwise, in the case of semi-infinite medium (Fig. 14) the hydraulic head loss H/f increases with the K_1/K_2 increase. Notice, however, that for cases when the lower layer has a greater permeability coefficient than the upper layer ($K_1/K_2 < 1$), most of the head loss is concentrated in the upper layer, resulting in greater pore water pressures. Consequently, the hydraulic head loss H/f decreases with the K_1/K_2 decrease.
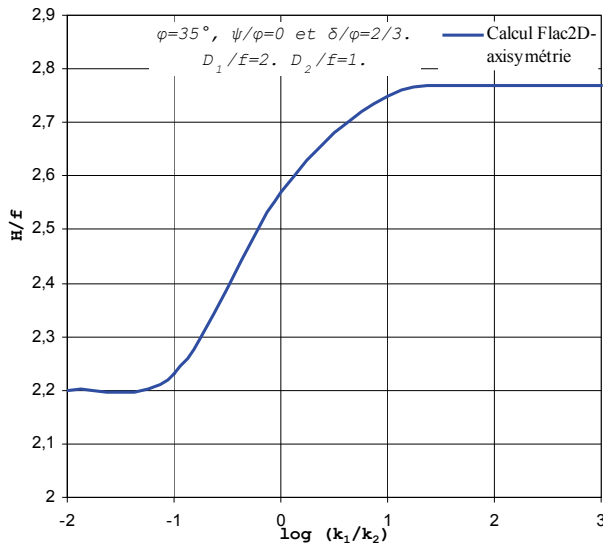

Fig. 12. H/f for various governing parameters $\varphi = 35°$, $\psi/\varphi = 0$ and $\delta/\varphi = 2/3$. $D_1/f = 2$, $D_2/f = 1$, for case A. Finite medium. $k_1/k_2 = 1/100$

In the case where the bottom of the sheet pile lies in the lower layer (case B), Fig. 13, and Fig. 14 ($D_1/f = 0.5$) for $K_1/K_2 > 100$, the head loss takes place solely in the lower layer, and the upper layer can be considered as a filter increasing the global stability of the soil in front of the sheet pile. Consequently, the increase of the hydraulic head loss with the K_1/K_2 increase is a logical phenomenon.
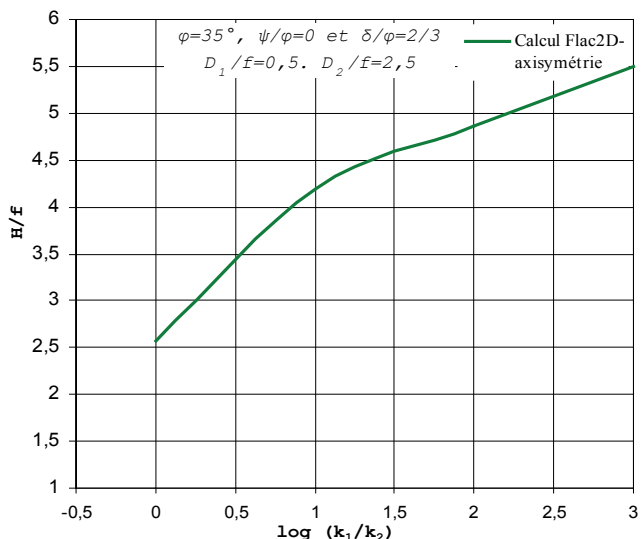

Fig. 13. *H/f* for various governing parameters $\varphi = 35°$, $\psi/\varphi = 0$ and $\delta/\varphi = 2/3$. $D_1/f = 0.5$, $D_2/f = 2.5$, for case B. Finite medium
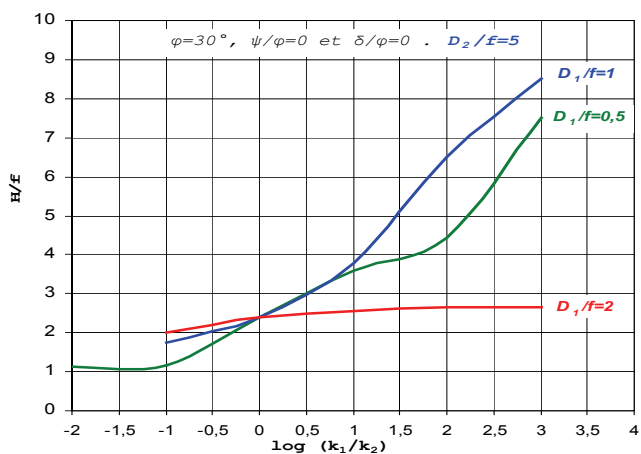

Fig. 14. *H/f* for various governing parameters $\varphi = 30°$, $\psi/\varphi = 0$ and $\delta/\varphi = 2/3$. $D_2/f = 5$. Semi-infinite medium

On the other hand, for cases when the lower layer has a greater permeability coefficient than the upper layer ($K_1/K_2 < 1$), most of the head loss takes place in the upper layer, resulting in a significant reduction of its resultant body force (buoyant weight + seepage force). Consequently, the hydraulic head loss H/f decreases with the K_1/K_2 decrease.

However, it should be noted that this calculation scheme is only valid as long as the vertical hydraulic gradient in the upper layer is smaller than the critical gradient $i_c = \gamma'/\gamma_w$, as otherwise failure by heaving of the upper layer will occur due to the fact that the saturated weight of this layer is equal to the resultant of the pore water pressures on the base of this layer. This limitation is shown in Fig. 13 and Fig. 14.

The analysis of results presented in Fig. 14 shows a high sensitivity of the critical pressure loss to the layer permeability contrast. The risk increases with the decrease of the thickness of the upper layer as well as its permeability. Indeed, for $D_1/f = 0.5$ a weak ratio of permeability $k_1/k_2 = 1/2$ reduces the critical head loss by 42%, wile a ratio of permeability $k_1/k_2 = 1/100$ reduces it by 43% compared to the value suggested by Terzaghi for homogeneous isotropic soil.

The comparison of these present axisymmetric case results (Fig. 14) to the two-dimensional case obtained by Benmebarek et al. (2005b) [11] is shown in Table 5.

Table 5

Critical hydraulic head loss H/f.
Case of isotropic two-layered semi-infinite soil medium

D_1/f	k_1/k_2	H/f	
		Flac2D	B
0.5	$1/100 \leq k_1/k_2 \leq 100$	1.12–4.42	1.13–4.46
1	$1/10 \ \leq k_1/k_2 \leq 10$	1.75–3.80	2.29–3.92
2	$1/10 \ \leq k_1/k_2 \leq 100$	2.00–2.65	2.69–2.77

B: after BENMEBAREK et al. (2005b) [11]

Hence, the values of critical hydraulic head loss H/f proposed in two-dimensions are overestimated, and thus the values of the safety factor are overestimated compared to the present axisymmetric case.

5. CONCLUSION

In this paper, the numerical finite difference method was applied to the zero effective passive earth pressure problem, taking into account the seepage flow due to dewatering. It showed that the failure mechanism, in the general case of axisymmetric *homogeneous* and *isotropic* hydraulic properties of the soil medium, is a boiling or

heaving. The present mechanism allowed us to determine the critical hydraulic pressure loss H/f corresponding to the zero effective passive pressures. For this case, the present mechanism describes the traditional heaving phenomenon in front of the sheet pile. The numerical results have shown that: (1) The heaving of a soil mass in front of the sheet pile occurs before the piping phenomenon in the case of a homogeneous and isotropic semi-infinite soil medium as long as φ is smaller than 45°; (2) H/f value causing failure increases with the decrease of the layer depth in the case of a single-layer problem; (3) H/f depends on the soil friction angle and the interface soil/wall friction; (4) the boiling appears only for dense and dilatant sand in which $\varphi \geq 35°$, $\psi/\varphi > 1/2$ and a rough wall $\delta/\varphi \geq 0$. In this case the exit gradient becomes equal to the critical hydraulic gradient, whereas heaving occurs for the other cases; (5) the soil dilation angle has a significant influence on the failure mechanism shape. For a dilating material, a triangular prism failure by heaving is obtained, whereas a rectangular prism for other cases. The rectangular prism obtained has a width smaller than that obtained in Terzaghi's method; (6) as the diameter of the cofferdam increases, the water height at failure increases.

The study of *anisotropy* effect on seepage failure has shown that: (1) the axisymmetric bottom stability against seepage failure always corresponds to a bulk heave and contrary to the isotropic case, boiling has not occurred; (2) the anisotropy of the permeability coefficient of the soil medium can induce a significant reduction of the critical hydraulic head loss causing failure; (3) H/f causing failure decrease with the decrease of the layer depth in this case of anisotropic single-layer problem; (4) the rectangular prism obtained has a width larger than that obtained in Terzaghi's method.

The study of the *two-layered* soil medium has shown that: (1) for great values of K_1/K_2, when the bottom of the sheet pile lies in the upper layer, one obtains the case of a single layer of limited depth, and when the bottom of the sheet pile lies in the lower layer, the upper layer can be considered as a filter; and for small values of K_1/K_2, most of the head loss takes place in the upper layer, thus resulting in a significant reduction of the effective passive pressures; (2) the failure mechanism shapes and the hydraulic head loss inducing failure are very sensitive to the layered permeability ratio. The risk of seepage failure by heaving increases with the decrease of the thickness of the upper layer as well as its permeability; (3) the values of critical hydraulic head loss proposed in two-dimensions are overestimated, and thus the values of the safety factor are overestimated.

Finally, one can see that the effect of *excavation shapes*; *soil anisotropy* and *non-homogeneity* is significant for the reduction of the critical hydraulic head loss H/f corresponding to the zero effective passive pressures. Thus, the assessment of H/f taking into account these parameters is of great interest in the practice of geotechnical engineering.

REFERENCES

[1] TERZAGHI K., *Theoretical soil mechanics*, Wiley, New York 1943.

[2] TERZAGHI K., PECK R.B., *Soil mechanics in engineering practice*, 2nd ed., John Wiley & Sons, New York 1948.

[3] MCNAMEE J., *Seepage into a sheeted excavation*, Géotechnique, The Institution of Civil Engineers, London, 1949, 4 (1), 229–241.

[4] MARSLAND A., *Model experiments to study the influence of seepage on the stability of a sheeted excavation in sand*, Géotechnique, The Institution of Civil Engineers, London, 1953, 4 (7), 223–241.

[5] DAVIDENKOFF R.N., *Zur berechnung des hydraulischen grundbruches*, Wasserwirtschaft, 1954, (46), 298–307.

[6] BAZANT Z., *Ergebnisse der Berechnung der Stabilitat gegen Hydraulischen Grundbruch mit Hilfe der Elektronen-Rechenan-lage*, Proc. of the Int. Conf. on Soil. Mech. and Found, Eng., Budapest, 1963, 215–223.

[7] DAVIDENKOFF R.N., FRANKE O.L., *Untersuchung der raumlichen Sickerstromung in eine umspundete Baugrube in offenen Gewassern*, Die Bautechnik, 1965, 9, 298–307.

[8] KASTNER R., *Excavations profondes en site urbain: Problèmes liés à la mise hors d'eau. Dimensionnement des soutènements butonnés*, Thesis of Docteur e's Sciences, INSA, France, 1982.

[9] KHAN M.R.A., TAKEMURA J., FUKUSHIMA H., KUSAKABE O., *Behaviour of double sheet pile wall cofferdam on sand observed in centrifuge tests*, IJPMG – Int. J. of Physical Modelling in Geotechnics, 2001, 4, 01–16.

[10] BENMEBAREK N., BENMEBAREK S., KASTNER R., *Numerical studies of seepage failure of sand within a cofferdam*, Elsevier, Computers & Geotechnics, 2005a, Vol. 32, No. 4, 264–273.

[11] BENMEBAREK N., BENMEBAREK S., KASTNER R., *A numerical analysis of seepage failure in stratified soils within a cofferdam*, Proc. of the 10th Int. Conf. on Civi., Struct. and Envir. Eng. Computing, Scotland, 2005b, Paper 258.

[12] WUDTKE R.B., *Failure Mechanisms of Hydraulic Heave at Excavations*, 19th Eurp. Young Geotech. Eng. Conf. 3–5 Sep, 2008, Győr, Hungary.

[13] HOULSBY G.T., *Forces on retaining walls by Sokolovskii's method, including varying porewater pressures*, undergraduate project report. Cambridge, Cambridge University Engineering Department, 1975.

[14] SOUBRA A.H., KASTNER R., *Influence of seepage flow on the passive earth pressures*, Proc. of the Int. Conf. on retaining structures, 1992, 67–76.

[15] SOUBRA A.H., KASTNER R., BENMANSOUR A., *Passive earth pressures in the presence of hydraulic gradients*, Géotechnique, ICE, 1999, 3(49), 319–330.

[16] BENMEBAREK N., BENMEBAREK S., KASTNER R., SOUBRA A.H., *Passive and active earth pressures in the presence of groundwater flow*, Géotechnique, ICE, 2006, Vol. 56, No. 3, 149–158.

[17] WANG J.J., LIU F.C., JI C.L., *Influence of drainage conditions on coulomb-type active earth pressure*, Soil Mech. & Found Eng., 2008, Vol. 45, No. 5.

[18] BAUER G.E., *Dewatering, hydraulic failure and subsequent analysis of a sheeted excavation*, Proc. of Int. Conf. on Case Histories in Geotechnical Eng., 1984, 1415–1421.

[19] TANAKA T., *Boiling occurred within a braced cofferdam due to two dimensionally concentrated seepage flow*, 3rd Int. Symp., geotech. aspects of underg const. in soft ground, 23–25 Oct. 2002, Toulouse, 33–38.

[20] TANAKA T., YOKOYAMA T., *Effects of jet grouting under sheet piles on seepage failure*, Geotechnical aspects of Underground Construction in Soft Ground, Bakker et al. (eds.), Taylor & Francis Group, London 2006, 923–937.

[21] TANAKA T., KUSAKA T., NAGAI S., HIROSE D., *Characteristics of Seepage Failure of Soil under Various Flow Conditions*, Proc. of the 19th Int. Offshore and Polar Eng. Conf., Osaka, Japan, June 21–26, 2009, 90–95.

[22] MIURA K., SUPACHAWAROTE C., IKEDA K., *Estimation of 3D seepage force inside cofferdam regarding boiling type of failure*, Proc. of the Geoteh. – Year 2000. Developments in Geotechnical Engineering, 2000, 371–380.

[23] BOUCHELGHOUM F., BENMEBAREK N., *Numeric forecasting of the deep circular excavation out flow and foundation stability*, Proc. AL-Azhar Eng. Ninth Int. Conf. (AEIC), Egypt, 2007.

[24] BOUCHELGHOUM F., BENMEBAREK N., BENMEBAREK S., KASTNER R., *A 3D numeric modelling of groundwater flow within circular cofferdams*, Int. Algerian J. of Technology, AJOT, (2008a), Vol. 01, No. 01, 79–91.

[25] LIU F.C., WANG J.H., ZHANG L.L., *Axi-symmetric active earth pressure for layered backfills obtained by the slip line method*, J. of Shanghai Jiaotong University (Science), 2008, Vol. 13, No. 5, 579–584.

[26] BOUCHELGHOUM F., BENMEBAREK N., BENMEBAREK S., *A three-dimensional numeric investigation of piping phenomenon and out flow within square cofferdams*, Proc. First Int. Conf. on Geosciences to the service of lasting development, 26–28 Nov. 2006, Tebessa, Algeria, 29–33.

[27] BOUCHELGHOUM F., BENMEBAREK N., *A 3D numeric forecasting of piping phenomenon and flow within rectangular cofferdams*, Proc 4th Int. Conf. on Water Resources in the Mediterranean Basin, Algeria, 2008b.

[28] SOUBRA A.H., REGENASS P., *Three-dimensional passive earth pressures by kinematical approach*, ASCE J. Geot. Geoenv. Eng., 2000, 969–978.

[29] BENMEBAREK S., KHELIFA T., BENMEBAREK N., KASTNER R., *Numerical evaluation of 3D passive earth pressure coefficients for retaining wall subjected to translation*, Elsevier, Computers & Geotechnics, 2008, Vol. 35, 47–60.

[30] CAI F., UGAI K., *Three-dimensional numerical investigation of piping for excavations in cohesionless soils*, Groundwater Eng. – Recent advances, Kono, Nishigaki & Komatsu (eds.), Swerts & Zeithlinger, 2003.

[31] CAI F., UGAI K., *Seepage analysis of two case histories of piping induced by excavations in cohesionless soils*, The First Inter. Conf. on Construction IT, Beijing, China, 2004, August 12th–14th.

[32] KIM D.S., LEE B.C., *Instrumentation and numerical analysis of cylindrical diaphragm wall movement during deep excavation at coastal area*, Marine Geores and Geotech., 2005, No. 23, 117–136.

[33] TANAKA T., MATSUURA R., *Blow-out soil particles during construction of a caisson type pile*, Groundwater Eng., Kono Nishigaki & Kamatsu (eds.), 2003, 139–145.

[34] FLAC2D. Fast Lagrangian Analysis of Continua, ITASCA Consulting Group, Inc, Minneapolis, 2005.

[35] CUNDALL P.A., HART R.D., *Numerical modeling of discontinua*, Eng. Comp., 1992, 9, 101–113.

[36] SLOAN S.W., RANDOLPH M.F., *Numerical prediction of collapse loads using finite element methods*, Int. J. Num. Anal. Methods Geomech., 1982, 6, 47–76.

[37] FRYDMAN S., BURD H.J., *Numerical studies of the bearing capacity factor N_c*, J. Geot. Geoenv. Eng., 1997, 123, 20–29.

[38] ERICKSON H.L., DRESHER A., *Bearing capacity of circular footings*, J. Geotech. Geoenviron. Eng., 2002, 128, 38–43.